Mon. Not. R. Astron. Soc. **323**, 517–528 (2001)

The 1997 hard-state outburst of the X-ray transient GS 1354−64/BW Cir

C. Brocksopp,[1★] P. G. Jonker,[2] R. P. Fender,[2] P. J. Groot,[2,3] M. van der Klis[2] and S. J. Tingay[4]

[1]*Department of Physics and Astronomy, Open University, Walton Hall, Milton Keynes MK7 6AA*
[2]*Astronomical Institute 'Anton Pannekoek' and Center for High-Energy Astrophysics, University of Amsterdam,0.5cmKruislaan 403, 1098 SJ Amsterdam, the Netherlands*
[3]*Harvard-Smithsonian Center for Astrophysics, 60 Garden Street, Cambridge, MA 02138, USA*
[4]*Australia Telescope National Facility, Paul Wild Observatory, Locked Bag 194, Narrabri 2390, NSW, Australia*

Accepted 2000 November 16. Received 2000 October 16; in original form 2000 July 19

ABSTRACT

We present observations of the 1997 outburst of the X-ray transient GS 1354−64 (BW Cir) at X-ray, optical and, for the first time, radio wavelengths; our results include upper limits to the linear and circular polarization for the radio data. The X-ray outburst was unusual in that the source remained in the low/hard X-ray state throughout; the X-ray peak was also *preceded* by at least one optical outburst, suggesting that it was an 'outside-in' outburst – similar to those observed in dwarf novae systems, although possibly taking place on a viscous time-scale in this case. It therefore indicates that the optical emission was *not* dominated by the reprocessing of X-rays, but that instead we see the instability directly. While the radio source was too faint to detect any extended structure, spectral analysis of the radio data and a comparison with other similar systems suggest that mass ejections, probably in the form of a jet, took place and that the emitted synchrotron spectrum may have extended as far as infrared wavelengths. Finally, we compare this 1997 outburst of GS 1354−64 with possible previous outbursts and also with other hard-state objects, both transient and persistent. It appears that a set of characteristics – such as a weak, flat-spectrum radio jet, a mHz QPO increasing in frequency, a surprisingly high optical/X-ray luminosity ratio, and the observed optical peak preceding the X-ray peak – may be common to all hard-state X-ray transients.

Key words: accretion, accretion discs – stars: individual: GS 1354−64 – X-rays: stars.

1 INTRODUCTION

Soft X-ray transients are a class of low-mass X-ray binaries in which instabilities in the accretion disc cause a sudden increase in mass accretion rate on to the compact object, resulting in an outburst (see, e.g., Charles 1998, and references therein). While reminiscent of the dwarf novae class of cataclysmic variables (Van Paradijs 1996), these outbursts occur with intervals typically 10–20 years and usually decline over several months (Tanaka & Lewin 1995; Van Paradijs & McClintock 1995), sometimes displaying secondary outbursts as they do so (e.g., the X-ray flux of GS 1124−684 rose again by a factor of ∼2 about 80 days after the initial outburst; see Tanaka & Shibazaki 1996, and references therein). In between outbursts the X-ray transients lie in a quiescent state, and this gives us an excellent opportunity to study the companion star.

Although these objects are frequently referred to as *soft* X-ray transients on account of their ultrasoft X-ray spectra during the outbursts, an increasing number of their outbursts do *not* show the soft component (e.g., GRO J1719−24; Van der Hooft et al. 1996). Instead, the power-law component dominates the energy spectrum, reminiscent of the low/hard X-ray state of the persistent source Cyg X-1. However, as the term 'hard X-ray transient' has previously been used to describe the Be star + neutron star binaries (which typically show hard X-ray spectra), we do not use this term here. It is important to note that the term 'low/hard state' is used for historical reasons, dating back to observations of Cyg X-1 during the 1970s – it is somewhat misleading, as its current definition (Van der Klis 1995) is based on spectral properties and the source flux need not necessarily be 'low'.

A large number of the X-ray transients have been classified as black hole candidate (BHC) X-ray binaries – where possible, the preferred method is to determine the mass function (e.g. Charles 1998, and references therein), but in a large number of cases a black hole nature has been suggested on account of the X-ray properties. Following the unification scheme for the X-ray power

★ E-mail: cb@astro.livjm.ac.uk

density spectra of neutron stars and BHCs proposed by Van der Klis (1994, 1995), the power spectra of BHCs can be sorted according to the mass accretion rate; this is thought to increase from the low/hard state, through the intermediate state and the high/soft state, up to the very high state (but see also Homan et al. 2001). During the low/hard state, strong band-limited noise is present. In this scheme, low-frequency ($\leq$1 Hz) quasi-periodic oscillations (QPOs) seen in the low/hard state are viewed as an aspect of the low/hard state noise. Recently, Psaltis, Belloni & Van der Klis (1999) reported correlations between the frequencies of QPOs and broad-band power spectral features of neutron star and black hole X-ray binaries.

Transitions between X-ray states have been observed during the rise and subsequently during the decay of an outburst for a number of sources [e.g., GS 1124−68 (Ebisawa et al. 1994) and GRO J1655−40 (Méndez, Belloni & Van der Klis 1998)]. Of particular interest is GX 339−4, in which the transition from low/hard to high/soft X-ray states and back again was clearly tracked at radio wavelengths, with radio emission strongly suppressed in the high/soft state (Fender et al. 1999; Fender 2001a).

Ground-based follow-up observations of X-ray transients have shown that outbursts also occur at optical and radio frequencies. A0620−00, GRO J1655−40, GS 2023+338 (V404 Cyg) and GS 1124−684 are examples of X-ray transients detected in all three wavelength regimes (Tanaka & Lewin 1995, and references therein); in particular, the X-ray, optical and radio behaviours for GS 2023+338 were correlated during the 1989 outburst (Han & Hjellming 1992), and it is interesting to note that during this outburst (as in the case of GS 1354−64) the source remained in the low/hard state (e.g. Tanaka & Lewin 1995).

The optical emission is thought to be the result of reprocessing of X-rays in the disc – the disc absorbs X-rays and re-emits them at lower energies, delaying the optical by a few seconds as reported by Hynes (1998) in the case of GRO J1655−40. The radio appears to be the result of beamed synchrotron emission taking place in relativistic ejections of material from the centre of the disc; this may be in response to additional material being transported through the disc by the instability, and so we might expect some correlation between the radio and the X-ray/optical behaviour. However, a comparison between the radio light curves of A0620−00, GS 1124−68 and GS 2000+25 suggests that their profiles depend on inclination angle, the number of ejections, the time between them, and their strength and speed (Kuulkers et al. 1999). Therefore, as the radio emission may be anisotropic in the observer's frame, unlike (presumably) X-ray and optical, we might instead expect that it is *not* observed to be so closely correlated with these two components as they are with each other.

1.1 GS 1354−64

On 1987 February 13, the ASM on board the *Ginga* satellite (Swinbanks 1987) discovered GS 1354−64, observing it until 1987 August (Makino et al. 1987). The X-ray data were well fitted by a soft disc blackbody component, with inner disc temperature of $\sim$0.7 keV, and a hard power law with photon index 2.1 (Kitamoto et al. 1990). These X-ray properties are common for X-ray transients during outburst (Tanaka & Lewin 1995), and hint at a black hole nature for the compact object. It was also observed in the optical during the outburst, yielding magnitudes of $V \sim 16.9$, $B \sim 18$ (Kitamoto et al. 1990). GS 1354−64 had not previously been observed in the radio.

The position of this source on the sky is consistent with the position of two other transient sources: Cen X-2 (Francey 1971) and MX 1353−64 (Markert et al. 1979). Cen X-2 was the first 'soft X-ray transient' discovered, and one of the brightest (Tanaka & Lewin 1995). The outbursts of MX 1353−64 (1972) and GS 1354−64 (1987 and 1997) reached much lower intensities and showed different X-ray spectral properties – if Cen X-2 and MX 1353−64 were the same source as GS 1354−64, then it must show at least four different states (Kitamoto et al. 1990). This is not unfeasible – e.g., GX 339−4 has been observed in four states, and Cyg X-1 in three (see Fender 2001a, and references therein) – it is therefore probable that these sources are indeed one and the same, in which case we note that the 1997 outburst was significantly sub-Eddington. The error circles for the positions of each 'source' can be found in Kitamoto et al. (1990). We investigate the nature of the various states further in Section 4.

GS 1354−64 was observed in outburst again in 1997 November. Preliminary results from the ASM on board the *Rossi X-ray Timing Explorer* (*RXTE*) showed a rise from 16 to 50 mCrab in the first half of November (Remillard, Marshall & Takeshima 1997); the BATSE instrument on the *Compton Gamma Ray Observatory* (*CGRO*) detected hard X-rays up to 200 keV which rose from 60 to 160 mCrab (Harmon & Robinson 1997). The optical and infrared counterparts were also detected with magnitudes of $R \sim 16.9$, $B \sim 18.1$ (November 22; Castro-Tirado, Ilovaisky & Peterson 1997) and $J \sim 15.35$, $K \sim 13.95$ (November 20; Soria, Bessell & Wood 1997). Optical spectroscopy during the decay revealed strong emission lines corresponding to Hα, Hβ and He II λ4686, plus weaker He I λ4471 and Hγ emission (Buxton et al. 1998). The Hα emission profile varied from single- to double-peaked over three nights of observations during the decay from outburst, indicating the presence of an accretion disc. The radio counterpart was detected at 2.5, 4.8 and 8.6 GHz with a flux of 1–3 mJy (November 24/25; Fender et al. 1997). No indication of the orbital period was detected at any wavelength.

A recent paper by Revnivtsev et al. (2000) gives an analysis of *RXTE*/ASM, HEXTE and PCA data during the outburst. Their work indicates that the X-ray energy spectrum is dominated by a power law, typical of X-ray binaries in the low/hard state. However, the fit is improved by the addition of a 6.4-keV iron line and a reflection component suggestive of the presence of an accretion disc; low-energy disc photons are upscattered by a Comptonizing corona to higher energies, resulting in the X-ray emission. Here we present *B*, *V* and *R* photometry and radio data from the outburst, combining it with further *RXTE*/PCA analysis and public ASM and *CGRO*/BATSE data.

2 OBSERVATIONS

We have obtained public *RXTE*/ASM, *RXTE*/PCA and *CGRO*/BATSE data for the 1997 outburst of GS 1354−64. Light curves for this and for our optical and radio data are shown in Fig. 1.

2.1 X-ray

The *RXTE* satellite observed GS 1354−64 ten times with the onboard proportional counter array (PCA; Jahoda et al. 1996). We present only the analysis of the first nine of these, since the count rates were too low and the observing time too short during the last observation to constrain our fit parameters. During the outburst a total of nearly 60 ks of good data was obtained. A log of the

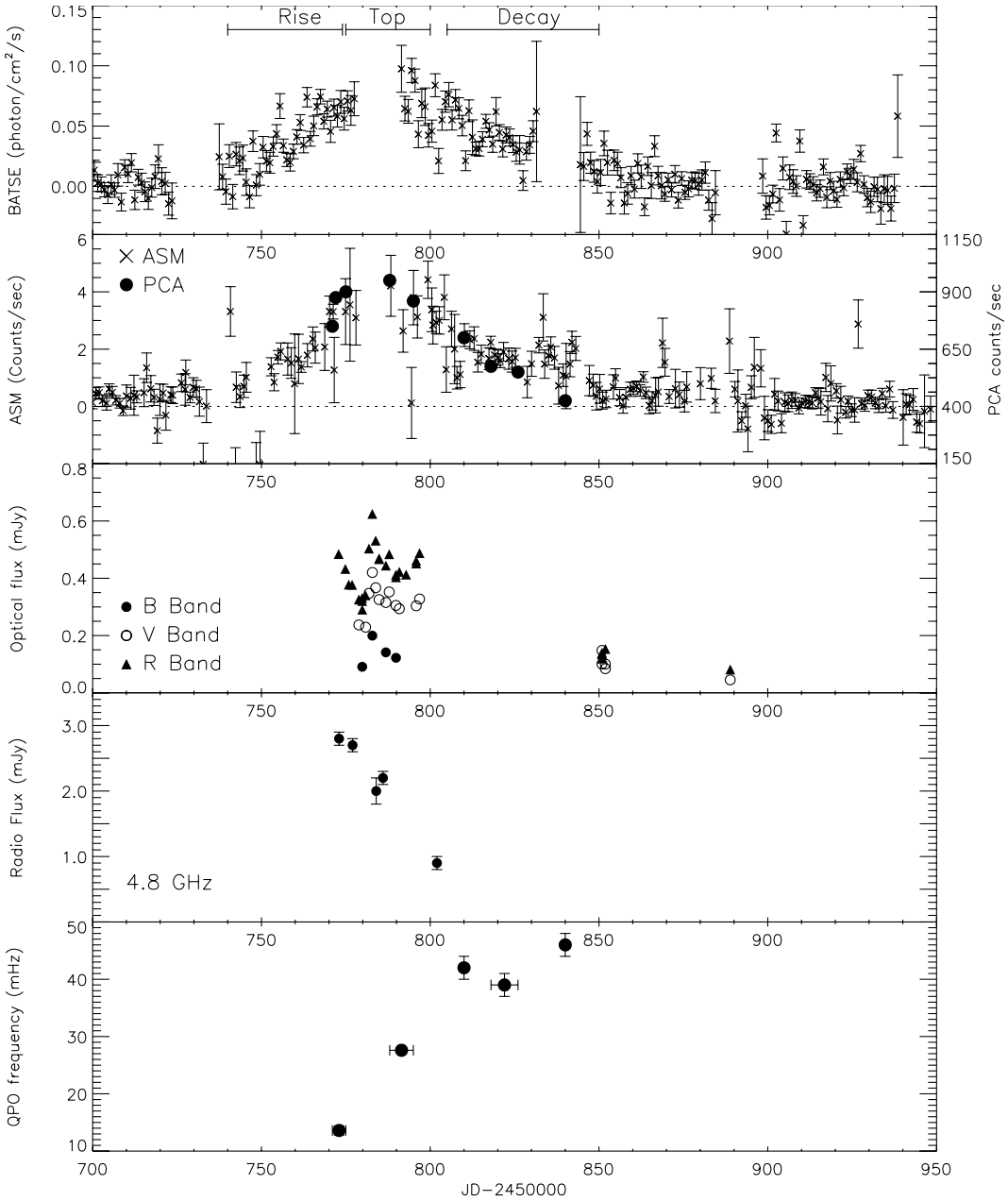

Figure 1. BATSE, ASM, PCA, optical and radio (4.8-GHz) light curves of the 1997 outburst for the period 1997 October 8–1998 May 16. Radio light curves at other frequencies are shown later in this paper. Error bars on the optical points are smaller than the symbols. The variability of the QPO frequency is also shown in the bottom panel.

observations which we present here (following background corrections) can be found in Table 1. During ∼4 per cent of the time only four of the five PCA detectors were active – when this was the case, the data were averaged. The count rates quoted are approximate, because they depend on the background model and can vary over an observation.

All the data were obtained in each of three modes. The Standard 1 mode has a time resolution of 1/8 s in one energy channel (2–60 keV). The Standard 2 mode has a time resolution of 16 s, and the effective 2–60 keV PCA energy range is covered by 129 energy channels. In addition, high time-resolution data (with a time resolution of 125 μs or better) were obtained for all observations in at least 64 energy channels covering the effective 2–60 keV PCA energy range.

Additional soft (2–12 keV) X-ray data have been obtained from the ASM on board *RXTE*; we use the public archive data from the web (http://xte.mit.edu). A detailed description of the ASM, including calibration and reduction is published in Levine et al. (1996). Our hard (20–100 keV) X-ray data came from the BATSE instrument on the *CGRO* and was processed using the standard BATSE Earth occultation software. Again, we have used the public archive data from the web. A detailed overview of the BATSE instrument can be found in Fishman et al. (1989).

2.2 Optical

The optical counterpart to GS 1354−64 was observed on 18 nights during 1997 November/December and two nights the

Table 1. Log of the *RXTE*/PCA observations. The penultimate column indicates the category of the observation (see text).

Number	Observation ID	Date	Total on source observing time (ks)	Category	Mean count rate (count s^{-1})
1	20431-01-01-00	1997-11-18	3.2	rise	~750
2	20431-01-02-00	1997-11-19	6.0	rise	~875
3	20431-01-03-00	1997-11-22	8.4	rise	~900
4	20431-01-04-00	1997-12-05	7.6	top	~950
5	20431-01-05-00	1997-12-12	6.4	top	~860
6	30401-01-01-00	1997-12-27	7.0	decay1	~700
7	30401-01-02-00	1998-01-04	7.7	decay2	~575
8	30401-01-03-00	1998-01-12	6.1	decay2	~550
9	30401-01-04-00	1998-01-26	7.1	decay3	~425

Table 2. Identifiers, coordinates (J2000 equinox) and magnitudes of the eight reference stars used in the photometry. The 'BJF' part of the identifier refers to Brocksopp et al. 2001 (this work).

Identifier, RA, Dec.	V (mag)	$B-V$ (mag)	$V-R$ (mag)
BJF J135807.07−644309.9	16.269 (0.005)	0.987 (0.016)	0.632 (0.006)
BJF J135807.94−644309.3	16.028 (0.004)	1.111 (0.013)	0.646 (0.005)
BJF J135815.53−644305.1	15.446 (0.002)	1.905 (0.014)	1.088 (0.002)
BJF J135814.93−644337.6	15.797 (0.003)	1.570 (0.015)	0.895 (0.003)
BJF J135813.21−644348.4	15.506 (0.002)	1.914 (0.015)	1.084 (0.002)
BJF J135809.39−644439.1	15.463 (0.003)	0.889 (0.006)	0.557 (0.003)
BJF J135807.71−644513.1	15.036 (0.002)	0.937 (0.005)	0.559 (0.002)
BJF J135811.48−644516.0	15.026 (0.002)	0.811 (0.005)	0.485 (0.002)

following February. Further observations taken a year later revealed no source, suggesting that the source in quiescence has $V \geq 22$ mag ($\leq$0.005 mJy). The 0.91-m Dutch telescope at the European Southern Observatory in Chile was used, equipped with a 512×512 TEK CCD and standard Johnson B and V, and Cousins R filters. Typical exposure times were 20 min in B and 5 min in V and R (although there were also some 10-min observations in all three bands).

The data were processed using routine bias subtraction and flat-field division in IRAF. Aperture photometry was applied, both to GS 1354−64 and to eight field stars; the coordinates of these stars are shown in Table 2. The photometry was then calibrated (also with IRAF) using photometric standard stars in the fields of PG 0231+051 and Mark A (Landolt 1992). Magnitudes are given in Table 3. The magnitudes were converted into mJy to ease comparison with the radio fluxes; Johnson conversions were used for the B and V bands, and Cousins conversions for the R band.

Table 3. Calibrated magnitudes for our optical photometry. Errors are given in parentheses.

JD−245 0000	B	V	R
772.87	–	–	16.89 (0.04)
774.86	–	–	17.02 (0.02)
775.86	–	–	17.16 (0.01)
776.86	–	–	17.17 (0.02)
778.86	–	18.02 (0.07)	17.32 (0.02)
779.84	–	–	17.34 (0.03)
779.85	–	–	17.30 (0.01)
779.86	19.18 (0.07)	–	17.45 (0.06)
780.85	–	18.06 (0.02)	17.28 (0.01)
781.85	–	17.61 (0.03)	16.85 (0.01)
782.84	18.32 (0.02)	17.40 (0.03)	16.62 (0.01)
783.84	–	17.55 (0.01)	16.79 (0.01)
784.85	–	17.68 (0.01)	16.93 (0.01)
784.86	–	–	16.93 (0.01)
786.86	18.70 (0.03)	17.71 (0.07)	16.99 (0.02)
787.85	–	17.59 (0.01)	16.89 (0.01)
789.85	–	–	17.07 (0.02)
789.85	18.85 (0.14)	17.75 (0.02)	17.09 (0.01)
790.84	–	17.79 (0.01)	17.04 (0.01)
792.85	–	–	17.07 (0.05)
795.84	–	17.75 (0.02)	16.95 (0.03)
795.84	–	–	16.97 (0.01)
796.84	–	17.67 (0.02)	16.89 (0.01)
850.88	–	–	18.41 (0.22)
850.88	–	18.95 (0.40)	18.28 (0.10)
850.88	–	–	18.29 (0.06)
850.88	–	18.53 (0.31)	18.24 (0.14)
851.89	–	18.95 (0.02)	18.14 (0.01)
888.88	–	19.82 (0.14)	18.83 (0.06)

2.3 Radio

Radio observations were made at the Australia Telescope Compact Array at 1.384, 2.496, 4.800 and 8.640 GHz at eight epochs during the period JD 245 0773 – JD 245 0802 (1997 November 20, 24, 25 and December 1, 2, 3, 4, 19). The array was in configuration 6C, which included the 6-km antenna, giving a nominal angular resolution of ~1 arcsec at 8.640 GHz. Standard flagging, calibration and imaging techniques were used within MIRIAD; the flux calibrator was PKS 1934−638, and the phase calibrator was PMN J1417−5950. The integration times for the first epoch totalled 2.5 h at each frequency; typical integration times for following epochs were <1 h, yielding reasonable S/N but unfortunately poor *uv* coverage (the *uv* plane is the projection of the antenna baselines on to the plane of the sky). As a result, for most epochs the synthesized beam from the observations was extremely elongated. Furthermore, the sparse *uv* coverage meant that the flux densities measured were a function of the cell size used in making the maps, as a result of different gridding in the FFTs. Both effects resulted in difficulty in measuring reliably the flux densities at the epochs with the shortest observations. In order

Table 4. ATCA observing log, and results of image-plane (naturally weighted) and *uv*-plane point-source fits to the data.

Date (JD − 245 0000)	Frequency (GHz)	Total Time (h)	Image-plane fit (mJy)	*uv*-plane fit (mJy)	Linear Pol. (3σ)	Circular Pol. (3σ)
773	1.384	2.5	2.6 ± 0.2	3.6 ± 0.1	<8%	<7%
	2.496		2.8 ± 0.1	2.9 ± 0.1	<9%	<8%
	4.800		2.8 ± 0.1	2.9 ± 0.1	<6%	<6%
	8.640		1.6 ± 0.1	1.9 ± 0.1	<15%	<16%
777–778	1.384	0.7	2.5 ± 0.5	2.3 ± 0.3		
	2.496		2.5 ± 0.1	3.7 ± 0.2		
	4.800		2.7 ± 0.1	3.7 ± 0.3		
	8.640		2.5 ± 0.1	2.2 ± 0.2		
784–785	2.368	0.58	3.5 ± 0.1	3.7 ± 0.3		
	4.800		2.0 ± 0.2	2.7 ± 0.2		
	8.640		1.5 ± 0.1	2.2 ± 0.3		
786–787	4.800	1.25	2.2 ± 0.1	3.1 ± 0.2		
	8.640		1.8 ± 0.2	3.9 ± 0.5		
802	4.800	0.75	0.9 ± 0.1	1.7 ± 0.4		
	8.640		1.1 ± 0.1	1.8 ± 0.4		

to improve the situation, we combined data from two adjacent days (for November 24/25, December 01/02 and 03/04), which significantly improved the *uv* coverage in all three cases. In addition, as well as performing point-source fits to the final (naturally weighted) images, we also performed point-source fits in the *uv* plane, thereby avoiding gridding errors. On December 3/4, data were collected in two adjacent bands, centred on 2.240 and 2.496 GHz respectively, and combined to improve the S/N by $\sqrt{2}$ at an effective frequency of 2.368 GHz.

In Table 4 we present the ATCA observing log and results of our image-plane and *uv*-plane fits to a point source. It is clear that both the image-plane and *uv*-plane results follow a similar trend, steadily declining by a factor of ∼2 in the month between November 20 and December 19. It is also clear that the spectrum is generally flat, especially at lower (≤4.800 GHz) frequencies. Between 4.800–8.640 GHz the spectrum appears to be initially optically thin, but gradually flattens until becoming inverted by the last detection on December 19. We note that the *uv*-plane fits invert one epoch earlier than those of the image plane.

3 RESULTS AND ANALYSIS

3.1 X-ray

The X-ray light curves in Fig. 1 have a triangular shape, as defined by Chen, Shrader & Livio (1997), with a possible secondary outburst during the decay at ∼JD 245 0835. It is clear from Fig. 1 that the soft and hard X-rays are well correlated – we obtain a value of 0.6 for the Spearman rank correlation coefficient between the daily averaged *RXTE*/ASM and *CGRO*/BATSE light curves, despite the poor S/N. We also note that the energy spectra of both X-ray bands are dominated by a power-law component (Harmon & Robinson 1997; Revnivtsev et al. 2000), which indicates a common origin, i.e., a Comptonizing corona which upscatters low-energy (optical and UV) disc photons to higher energies (e.g. Van Paradijs 1998). This is significantly different from the 1987 outburst, when the X-rays showed a soft disc blackbody spectrum (Kitamoto et al. 1990). In the 1997 outburst the presence of an accretion disc can be inferred only indirectly, with the inclusion of a reflection component in the soft X-ray spectrum (Revnivtsev et al. 2000).

For all *RXTE*/PCA observations we calculated power spectra with a Nyquist frequency of 512-Hz using data segments of 512-s length each in one combined broad energy band ranging from 2–60 keV. To characterize the power spectra (1/512–512 Hz) we used a fit function consisting of a broken power law, plus a Lorentzian with its frequency fixed at 0 Hz to describe the low-frequency noise component. We also included a second Lorentzian to describe the QPO on top of the noise component. The frequency of the noise Lorentzian became negative when it was treated as a free parameter. Errors on the fit parameters were determined using $\Delta\chi^2 = 1.0$ (1σ single parameter). Power arising in the power spectrum due to Poisson noise has been subtracted – this also takes deadtime into account. The fit to the normalized (Belloni & Hasinger 1990) power spectrum of observations 4 and 5 combined is shown in Fig. 2.

We divided the outburst into three parts on the basis of the X-ray light curve: the rise, the top, and the decay (see Table 1 and Fig. 1). The decay observations were further subdivided into three parts in order to follow the changes in the fit parameters during the decay of the outburst.

The properties of our fit parameters are given in Table 5. We detect a QPO at low frequencies; its frequency increased from 13.6 ± 0.8 mHz at the rise to 46 ± 2 mHz at the end of the decay. The FWHM also increased over this range from 4.4 ± 1.5 mHz to 11^{+10}_{-4} mHz. The break frequency increased gradually from 56 ± 5 mHz during the rise to 110 ± 10 mHz during the last part of the decay. The power-law index at frequencies below the break frequency changed from 0.59 ± 0.07 during the rise to 0.100 ± 0.001 at the top; during the decay it varied between 0.22 ± 0.07 and $(-3 \pm 5) \times 10^{-2}$. At frequencies above the break frequency the power law became gradually steeper, with indices of 1.46 ± 0.01 during the rise to 1.9 ± 0.1 during the last part of the decay.

The increasing of the frequency at which the QPO and break occur suggests that the inner radius of the disc is decreasing as the outburst takes place (Revnivtsev et al. 2000). A general softening of the spectrum, consistent with this geometry, was also observed, and was seen previously in GS 1354−64 by Kitamoto et al.

(1990). A similar increase in frequency of low-frequency QPOs was discovered during an outburst of the X-ray transient GRO J1719−24 by Van der Hooft et al. (1996). If the increasing frequencies of the QPOs really do relate to the inner disc, then it is interesting to note that the inner disc radius does not appear to increase again during the decay from outburst.

From the high fractional rms amplitude of the low-frequency noise throughout the outburst, the hard spectrum (Revnivtsev et al. 2000) and the relatively low intensity increase [compared with the outbursts of Cen X-2 (Francey 1971) and MX 1353−64 (Markert et al. 1979) – we investigate this further in Section 4] we conclude that the source was in the low/hard state during the entire outburst (see Van der Klis 1995). This is unusual, as the majority of X-ray transients enter the high/soft state during outbursts; known exceptions include GRO J0422+32 (e.g. Sunyaev et al. 1993), GRO J1719−24 (e.g. Van der Hooft et al. 1996) and GS 2023+338, although in the last case it is possible that the system was in a soft but absorbed state at its peak, then returning to the low/hard state (Życki, Done & Smith 1999).

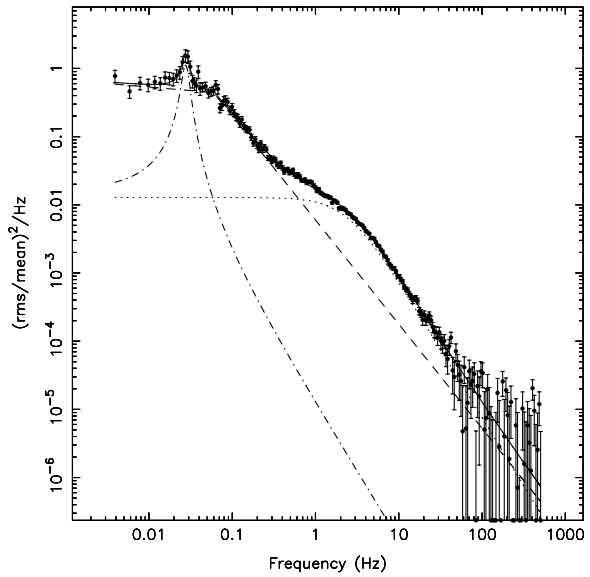

Figure 2. Normalized (Belloni & Hasinger 1990) power spectrum of observations 4 and 5 combined. The power arising in the power spectrum due to Poisson noise has been subtracted. The solid line represents the best fit to the data. This best-fitting function is built up by three components. The dashed line represents the contribution of the broken power-law component, the dotted line represents the contribution of the Lorentzian component with its frequency fixed at 0 Hz, and the dot-dashed line represents the contribution of the Lorentzian used to represent the QPO.

While the increase in QPO frequency and in break frequency during the decay of the outburst is *not* a common feature of BHCs whilst in the low/hard state, it appears that it *is* a typical feature during the *outbursts* of X-ray transients (see Section 4). Observations of the persistent BHCs during *transitions* from the low/hard to the high/soft state would be useful to determine whether or not the QPO frequency increases at these times – *RXTE* observations of the 1996 Cyg X-1 transition to the soft (intermediate?) state suggest that although a mHz QPO was present and the frequency certainly varied, it was not simply a frequency increase during the transition (Cui et al. 1997).

3.2 Optical

Our optical observations show that the X-ray increase was accompanied by an optical outburst reaching $B \sim 18.3$, $V \sim 17.3$ and $R \sim 16.6$ mag at maximum. As is typical for X-ray transients (e.g. Van Paradijs & McClintock 1995, and references therein), the subsequent decline was considerably longer than that of the X-rays, taking at least 120 d. Further observations a year later revealed no source, suggesting that there had been a brightening of $\geq$5 mag above the quiescent level.

The photometry suggests that the optical and X-ray events were not as well correlated as would be expected in a 'normal' soft X-ray transient event, in which the dominant source of optical emission would be reprocessing of X-rays. Indeed, whereas the X-rays produce a gradual rise and decay, the optical photometry appears to peak at least three times. The three apparent peaks are labelled in Fig. 3.

The first 'peak' occurs prior to our observations, but can be inferred from the *R*-band decline at the beginning of the data set. The X-rays have begun to rise by this point, but there is still a $\geq$10-d delay after our initial *R* band observations before the X-ray peak is reached. This optical peak is unlikely to be the result of reprocessing of soft disc X-rays on account of the low X-ray flux and the lack of evidence for a disc component in the X-ray energy spectrum. [It is not impossible, despite the lack of correlation; e.g., GRO J1655−40 shows an anticorrelated X-ray/optical outburst, but echo mapping shows that reprocessing of X-rays is still the dominant contributor to the optical flux (Hynes et al. 1998).]

A similar phenomenon is seen in dwarf novae – as the disc instability moves inwards from the outer parts of the disc, the outburst is seen first in the optical and then in the ultraviolet. While it is feasible that this phenomenon occurs also in X-ray transient events, it has rarely been observed (e.g., GRO J1655−40; Orosz 1997). If this is the case for this outburst of GS 1354−64, then our data suggest that the instability takes $\geq$10 d to cross the disc and peak in the X-rays. This is not

Table 5. Properties of the two Lorentzians and the broken power-law component. The frequency of the noise component was fixed at 0 Hz.

Category	Rise	Top	Decay1	Decay2	Decay3
rms QPO (%)	10 ± 2	10 ± 1	10 ± 2	10 ± 2	9 ± 2
FWHM QPO (mHz)	4.4 ± 1.5	7 ± 1	11^{+11}_{-6}	19 ± 7	11^{+10}_{-4}
$\nu_{\rm QPO}$ (mHz)	13.6 ± 0.8	27.6 ± 0.6	42 ± 2	39 ± 2	46 ± 2
rms noise (%)	23.1 ± 0.2	22.1 ± 0.2	21.8 ± 0.5	24.1 ± 0.3	25.7 ± 0.5
FWHM noise (Hz)	3.84 ± 0.06	4.87 ± 0.07	5.1 ± 0.1	4.8 ± 0.1	4.6 ± 0.2
rms break (%)	33.4 ± 0.6	27.7 ± 0.4	27.3 ± 0.7	26.3 ± 0.4	26.8 ± 0.8
$\nu_{\rm break}$ (mHz)	56 ± 5	60 ± 4	91 ± 7	96 ± 4	110 ± 10
α ($\nu < \nu_{\rm break}$)	0.59 ± 0.07	0.100 ± 0.001	0.12 ± 0.05	$(-3 \pm 5) \times 10^{-2}$	0.22 ± 0.07
α ($\nu > \nu_{\rm break}$)	1.46 ± 0.01	1.53 ± 0.03	1.55 ± 0.05	1.82 ± 0.05	1.9 ± 0.1

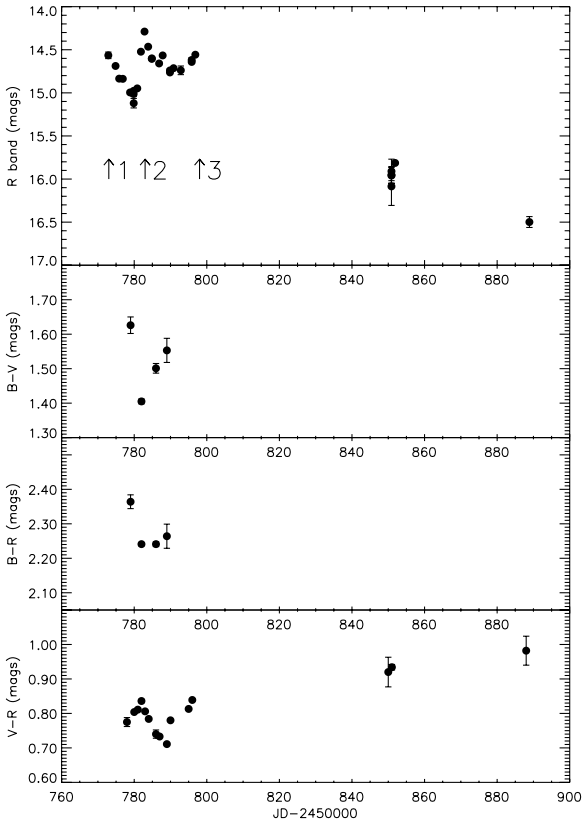

Figure 3. Dereddened R-band photometry [corrected for interstellar extinction using $E(B-V) \sim 1$ (Kitamoto et al. 1990) and the A_λ/A_V relations of Cardelli, Clayton & Mathis (1989)] and $B-V$, $B-R$ and $V-R$ colour evolution (instrumental magnitudes were used to determine colours in order to minimize errors). Arrows on the R-band plot indicate the three apparent peaks in the photometry.

impossible – Orosz calculates an optical lead of 6 d – but would place fairly large lower limits on the size of the orbit and/or donor star, and would also suggest that the instability moves on a viscous time-scale, unlike the thermal instabilities of the dwarf novae. The outburst of GRO J1655−40 was different from that of GS 1354−64 in that it reached the high/soft state (possibly the very high state; Méndez et al. 1998), it was considerably more luminous at all wavelengths, and the profiles of its rise to maximum in the BATSE and ASM data for GRO J1655−40 were considerably longer. In particular, the hard X-ray rise occurred ∼30 d after the soft X-rays – a phenomenon not seen in the case of GS 1354−64, where the ASM and BATSE data appear well correlated on account of both X-ray bands being dominated by the power-law component. GRO J1655−40 may therefore not be a suitable system with which to compare GS 1354−64.

The second peak (and only peak for which both the rise and decay were observed) took place during the 'top' period of the X-ray light curve (∼JD 245 0784) and was observed in all three optical bands. Without full X-ray coverage and better S/N in the X-ray bands it is not possible to say whether there is any evidence for correlated X-ray/optical behaviour. There is the hint of a small decline in the X-rays coincidentally with the decay of this second optical peak, but the S/N does not allow us to be conclusive. If the optical and X-ray were correlated, then we might assume that the second optical peak was produced by the reprocessing of X-rays (although the hard X-ray energy spectrum suggests that this is unlikely); a non-correlation would suggest that a second instability had passed through the optical-emitting regions of the disc.

The V and R bands also suggest the presence of a third rise in the light curve, ∼15 d after the time of the first maximum; it may also be hinted at in the X-rays, although a more significant secondary X-ray outburst takes place during the decay around JD 245 0835. These small secondary maxima during the decay of an outburst are commonly seen in X-ray transients (e.g., GRO J0422+32; Callanan et al. 1995), and may be due to additional, smaller instabilities.

Using the reddening correction determined by Kitamoto et al. (1990), $E(B-V) \sim 1$, and the A_λ/A_V relations of Cardelli et al. (1989), we have corrected our photometry for interstellar extinction ($A_B \sim 4.1$, $A_V \sim 3.1$, $A_R \sim 2.3$). In Fig. 3 we plot dereddened R-band magnitudes and the intrinsic colour evolution over time. To minimize errors, the colours have been determined from our original instrumental differential magnitudes.

We have no colour information for peak 1, but the $B-V$, $B-R$ and $V-R$ colours for peak 2 all hint at being anti-correlated with the photometric light curve, although there may be a delay of ∼0.5 d in the case of the latter. (Alternatively, it is possible that the $V-R$ colours are actually anticorrelated with the other colours, in which case there must be an additional contribution to $V-R$ from some other component, perhaps the jet.) The colours also suggest that the source became bluer during the rise to peak 2; this could be explained by a disc instability moving inwards, as the temperature and density of the disc will be increasing inwards. On the decay from peak 2 the colours redden, consistent with the disc cooling. We notice that the $B-V$ and (to a lesser extent) the $B-R$ colours vary more significantly than $V-R$; this suggests that, while the whole disc is brightening, the hot inner regions do so in particular, and this causes a greater brightening in the B band than the other two. This would be expected, and it shows that at shorter wavelengths the disc spectrum dominates the optical emission. Clearly, improved coverage of future outbursts would be extremely beneficial in order to test these possibilities.

Although we have only one pair of B-band/ASM points (and these are separated by 1.5 d), we also calculate the ratio of X-ray to optical luminosity, $\xi = B_0 + 2.5 \log F_x(\mu\mathrm{Jy})$, where B_0 is the extinction-corrected B magnitude, and F_x is the X-ray flux (Van Paradijs & McClintock 1995). Assuming $E(B-V) \sim 1$, an interstellar extinction (A_B) of 4.1 mag and 1 Crab ∼ 75 count s^{-1} (*RXTE*/ASM) ∼ 1060 μJy, we obtain a value of $\xi = 19$. This is slightly lower than that of other X-ray transients, indicating that the source might be underluminous in the X-rays – typically, $\xi = 22$ (±1). We note that during the 1987 outburst the ratio was calculated to be ∼16. This is surprisingly low and was thought likely to be due to errors in the reddening corrections and/or non-simultaneity of the observations (Van Paradijs & McClintock 1995). During the 1997 outburst it appears that the optical emission was dominated by the viscous instability moving through the disc, with minimal reprocessing. Other potential sources for the optical excess are synchrotron emission from the jet and/or a possible contribution due to irradiation of the companion star, although this may be insignificant, given the low magnitude of the source in quiescence.

3.3 Radio

We have observed the radio counterpart to GS 1354−644 for the first time. Detected at 1.384, 2.496, 4.8 and 8.64 GHz, it is a weak

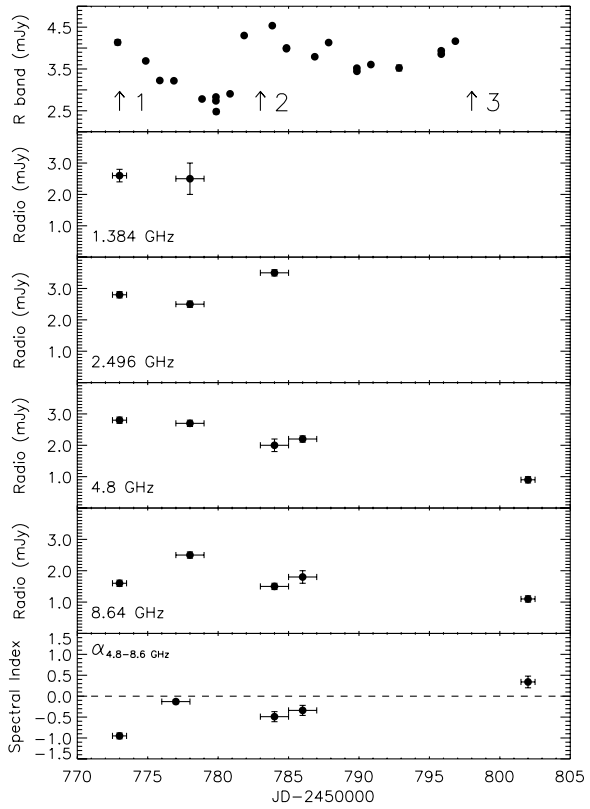

Figure 4. The *R*-band photometry and radio light curves at 1.4, 2.5, 4.8 and 8.6 GHz on an expanded scale. Evolution of the spectral index (α) at 4.8 and 8.6 GHz is shown in the bottom panel. Arrows on the *R*-band plot indicate the three apparent peaks in the optical photometry.

Table 6. The spectral index calculated for each epoch of our radio observations. Only the 4.8- and 8.6-GHz data have been used, so as to be consistent at every epoch.

JD−245 0000	α	error
773	−0.95	0.07
777/8	−0.13	0.05
784/5	−0.49	0.12
786/7	−0.34	0.12
802	0.13	0.14

source of 1–3 mJy, and our radio maps show no evidence for extension – combining data from the first two epochs suggests that the upper limits to the source extension are 11.2, 6.9 and 4.9×10^3 au at 2.5, 4.8 and 8.6 GHz respectively, assuming a distance of ∼10 kpc (Kitamoto et al. 1990). This is not really surprising, given such a low flux and the rather short exposure times of our observations. We have also determined the radio position of GS 1354−644 by assuming a point source and fitting a Gaussian – by assuming an error of 200 mas on the position of the phase calibrator we calculate the position of GS 1354−644 to be RA $13^h58^m09\overset{s}{.}7$, Dec. $-64°44'05\overset{''}{.}8$ (±200 mas) at 4.8 GHz – the positional error is dominated by the uncertainty in the absolute coordinates of the phase calibrator.

Light curves at all four observing frequencies are shown in Fig. 4. Surprisingly, the radio frequencies are not well correlated with each other – although they all seem to follow similar trends, in that some rise has taken place prior to our observations and a second rise may have occurred just after the second optical peak. Exact time differences cannot be measured, as each radio point contains data spanning up to two days. The lack of correlation with the X-rays and optical photometry is perhaps surprising, and possibly due either to our lack of data coverage or to reasons given by Kuulkers et al. (1999). Each maximum is probably associated with an ejection event as seen in, e.g., A0620 − 00 (Kuulkers et al. 1999).

While we would expect a certain frequency dependency in the relative delays and luminosities for these ejection events, the lack of obvious correlation is surprising. Correlated radio/optical behaviour has been observed previously (e.g., GS 2023+338; Han & Hjellming 1992), and it is possible that had we better radio coverage and/or S/N, then the same might be true here for all radio frequencies.

Fig. 4 also shows the evolution of the spectral index ($S_\nu \propto \nu^\alpha$, where α is the spectral index, ν is the frequency, and S_ν is the flux density at ν in mJy) over the period of our observations. The spectral indices are also tabulated in Table 6, and were determined by fitting the above power law to the data at 4.8 and 8.6 GHz – the other frequencies were not used to calculate the spectral index, as they were not measured at every epoch. Clearly, α is generally negative, particularly at the first epoch, corresponding to optically thin synchrotron emission. The spectrum becomes inverted at the final epoch, which is probably consistent with a partially self-absorbed continuous jet as seen in Cyg X-1 and GX 339−4 – it seems that this spectrum inversion is a typical feature of the jets of low/hard state systems (e.g. Fender 2001a, and references therein). Alternatively, the spectrum inversion could be indicative of a plasmon ejection emitting optically thick synchrotron emission, which will evolve to optically thin at successively lower frequencies as the plasmon expands (see, e.g., Kuulkers et al. 1999 for further evidence of this phenomenon) – however, this is more typically seen in *soft* X-ray transient outbursts. We note that using the *uv*-plane fluxes from Table 4 results in the spectrum inverting one epoch earlier.

By combining data from adjacent epochs, we have improved the S/N sufficiently to measure upper limits to the linear and circular polarization. These limits are determined from fits to the image plane, with percentages calculated as a fraction of the (image plane) total flux density; they can be found in Table 4. It is interesting to note that linear polarization of the soft X-ray transient 4U 1630−47 (flux density ∼0.5–3 mJy) was detected at 27 per cent, i.e., a level that we would have picked up had it been the case for GS 1354−64 (Hjellming et al. 1999). However, observations of GS 2023+338 (Han & Hjellming 1992) and GX 339−4 (Corbel et al. 2000) in the *hard* state yielded linear polarizations of 1–4 per cent, and this may turn out to be a value common to the hard state sources (which are probably partially self-absorbed).

While our optical investigation has suggested that the optical emission is the result of one or more heating waves travelling inwards through the disc, it is also interesting to note that the optical fluxes are comparable with those of the radio, suggesting that the flat spectrum associated with the central radio source might extend to higher frequencies. A flat synchrotron spectrum beyond the radio regime has been seen in a number of X-ray binaries in the low/hard X-ray state, e.g., Cyg X-1 to mm wavelengths and GRS 1915+105 to the infrared (Fender et al. 2000). It is therefore feasible that there may be a contribution to the optical emission from the jet; with the possible correlation between the optical and the radio this would not be surprising.

To investigate this further, we plot the extinction corrected spectrum for our optical data, plus the published infrared (*J* and *K* band) points of Soria et al. (1997) and the radio fluxes quoted in Table 4 which are from the same epoch as the infrared (Fig. 5). We have also extended the spectrum down to 843 MHz, with the inclusion of a data point from the Molonglo Observatory Synthesis Telescope (MOST) (Hunstead & Campbell-Wilson, private communication). This plot indicates that while the *B*- and *V*-band data are too bright to be associated with the radio, the *R*-band and the infrared points seem to lie approximately in a straight line – the best-fitting spectral index to the radio, infrared and *R*-band points is 0.004 ± 0.01, which is consistent with flat synchrotron emission up to the near-infrared. In contrast to this, the optical data alone yield a spectral index of 1.12–1.68, depending on the epoch, and the *B* and *V* data alone yield $\alpha \sim 0.02$–0.97. With a theoretical thermal disc spectrum (with no irradiation) of $S_\nu \propto \nu^{1/3}$ (e.g. Frank, King & Raine 1992, and references therein) it is probable that there is some additional optical component causing the steeper optical spectrum at some epochs. However, we note that without full coverage of the spectrum through the submm and infrared regimes we cannot be certain that the spectrum really is flat from radio to near-infrared.

We note that the 8.64-GHz point is somewhat discrepant. While it is possible that there is some systematic error due to the poor *uv* coverage, we point out that it may take some time after the ejection for the spectrum to invert, i.e., become dominated by a steady self-absorbed flow. For example, the radio spectrum of V404 Cyg did not invert until ∼25 d after the initial (hard state) outburst (Han & Hjellming 1992; Fender 2001b).

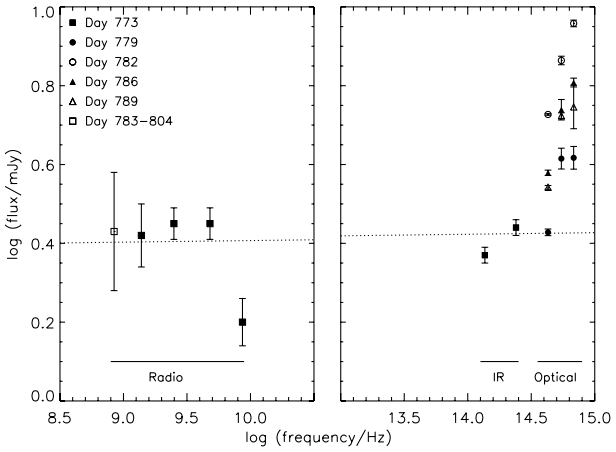

Figure 5. Spectrum ranging from radio through to optical. We include the infrared (*J*- and *K*-band) points of Soria et al. (1997) and the MOST data of Hunstead & Campbell–Wilson (private communication). Optical and infrared data have been corrected for interstellar extinction using a reddening estimate of $E(B-V) = 1$ (Kitamoto et al. 1990) and values of A_λ/A_V from Cardelli et al. (1989). The dotted line is the best-fitting straight line through the radio, infrared and *R* band ($\alpha \sim 0.004$).

4 COMPARISON WITH OTHER OUTBURSTS

4.1 Previous (possible) outbursts of GS 1354−64

We summarize the four possible outbursts of GS 1354−64 in Table 7. It is clear that the characteristics (i.e., the spectrum and luminosity) of each outburst are very different – Kitamoto et al. (1990) concluded that for GS 1354−64 to have produced all three outbursts known by that date, the source must show four distinct X-ray states, i.e., very high, high/soft, low/hard and faint/off states. Though less bright, the 1997 outburst appears to show a similar state to that of the 1972 event reported by Markert et al. (1979). However, as Kitamoto et al. demonstrate, the error boxes of the various satellites which may have detected GS 1354−64 cover a large area on the sky; if the system were to enter another 'Cen X-2 type' outburst, then it would confirm that the source can indeed display such a wide range of X-ray spectral behaviour – it may then be possible to confirm whether or not the three sources are one and the same.

4.2 Other X-ray transients reaching only the hard state

An increasing number of supposed 'soft' X-ray transients have been shown to remain in the low/hard X-ray state, the X-ray spectra showing little contribution from a soft disc component – although note that in some of these systems the fluxes (both X-ray and optical) were not at all 'low'. A list of hard-state X-ray transients can be found in Table 8. In comparing these five objects a number of trends can be seen, some of which may turn out to be indicative of low/hard-state outbursts of the X-ray transients.

We find that an increase in QPO frequency, a flat (or inverted) synchrotron radio spectrum and an over-bright optical counterpart (i.e., a surprisingly high optical/X-ray luminosity ratio; see Van Paradijs & McClintock 1995) may be properties common to the low/hard-state X-ray transients – although not exclusively so, as an increase in QPO frequency appears to be a common feature of the soft X-ray transients also (e.g., GS 1124 − 68; Van der Klis 1995) – however, it should be noted that the QPOs detected in the soft state tend to occur at higher frequencies. It is rare for the onset of a soft X-ray transient event to be observed in the optical, but at least two of these low/hard-state events have been observed to peak in the optical before the X-ray, suggesting that something other than reprocessing of X-rays dominates the optical emission. While these trends are clearly tentative, we note that none of these systems provides an exception to the 'rule' – either they follow the trends or there have been insufficient observations to determine either way.

There is a sixth source, Aql X-1, which also shows some (but

Table 7. Comparison between outbursts of Cen X-2, MX 1353−64 and GS 1354−64, which may all be the same source. X-ray peaks are quoted for the 1–10 keV range. See Tanaka & Lewin (1995, and references therein).

Source	Date	Duration (months)	Soft X-ray Peak (mCrab)	X-ray State	Optical Peak (mags)
Cen X-2	1966–1967	∼8	∼8000	(Very?) high/soft	$V<13.5$ (WX Cen)?
MX 1353−64	1972	∼11	75	low/hard	–
GS 1354−64	1987	∼6	≥300	high/soft	$V\leq16.9$ (BW Cir)
GS 1354−64	1997	∼5	50	low/hard	$V\leq17.3$ (BW Cir)

Table 8. Comparison between the five BHC X-ray transients which have remained in the low/hard state throughout an outburst.

Source	Date	X-ray Spectrum	mHz QPO During Outburst?	Radio Spectrum	Optical Peak Preceding X-ray Peak?	Optical/X-ray Luminosity Ratio
GS 1354−64	1997	low/hard	ν increases	flat→inverted	Yes	optically bright
GS 2023+338	1989	[1]low/hard (mostly?)	?	[2]flat→inverted	[3]Yes	[4]optically bright
GRO J0422+32	1992	[5]low/hard	[6]mHz QPO present	[7]flat→inverted	[8]Possibly*	? (no soft X-ray obs.)
GRO J1719−24	1993	[9]low/hard	[9]ν increases	[10]flat	?	? (no soft X-ray obs.)
XTE J1118+480	2000	[11]low/hard	[12,13]ν increases	[14]inverted	?	[15]optically bright

1. Tanaka & Lewin (1995)
2. Han & Hjellming (1992)
3. Chen, Shrader, Livio (1997)
4. Van Paradijs & McClintock (1995)
5. Van der Hooft et al. (1999)
6. Kouveliotou et al. (1992)
7. Shrader et al. (1994)
8. Callanan et al. 1995)
9. Van der Hooft et al. (1996)
10. Hjellming et al. (1996)
11. Hynes et al. (2000)
12. Yamaoka et al. (2000)
13. Wood et al. (2000)
14. Dhawan et al. (2000)
15. Garcia et al. (2000)

*The optical peak *appeared* to precede that of the BATSE data, but coverage was insufficient to be conclusive.

not all) of these trends – it has been omitted from Table 8 as it is a neutron star X-ray transient, its X-ray spectral properties classifying it as an atoll source (Cui et al. 1998; Reig et al. 2000). However, Aql X-1 has been observed to peak in the optical before the soft X-rays (Shahbaz et al. 1998), and it also demonstrates an increase in QPO frequency throughout the outburst (Cui et al. 1998). It should, however, be pointed out that the QPOs seen in Aql X-1 are found at kHz frequencies rather than the mHz QPOs found in the tabulated sources. Consequently, it may be incorrect to compare them, but see also Psaltis et al. (1999). Unlike the BHC systems, there is no optical excess. Although there was a weak radio counterpart to the outburst (Hjellming, Han & Roussel-Dupre 1990), there was no spectral information – Aql X-1 is currently one of only a small number of atoll sources for which radio counterparts have been detected.

It is also worth comparing these five sources with the low/hard states of persistent black hole X-ray binaries. While mHz QPOs have been reported in these systems (e.g. Vikhlinin et al. 1994, and references therein), a variable QPO frequency is not a typical feature of the low/hard state for these systems, and so it may seem surprising that we see it here. However, although the transients remain in the low/hard state, the change in QPO suggests that the inner disc radius is decreasing – it therefore appears that the transition to the soft state is initiated but not completed. Therefore this increase in QPO frequency should probably be considered a feature of the *transition*, rather than of the state itself – this would be consistent with the inner radius of the disc changing during the transition but remaining constant once a stable X-ray state is reached. This theory could be easily tested for the persistent sources during a transition, although *RXTE* observations of the 1996 transition of Cyg X-1 suggest that it may not be just a simple increase in frequency with flux (Cui et al. 1997) – further investigation of this would be useful. The radio behaviour of the persistent sources is very similar to that of these five transients – for example, Cyg X-1 (Brocksopp et al. 1999) and GX 339−4 (Corbel et al. 2000) both emit flat spectrum jets whilst in the low/hard state (see also Fender 2001b for comparison between the radio properties of persistent and transient sources in the low/hard state). This jet is quenched on reaching the soft state – this is probably also the case for soft X-ray transients, although the material ejected during the state transition will continue to produce bright radio emission, despite being physically decoupled from the accretion process (e.g., A0620−00; Kuulkers et al. 1999).

5 DISCUSSION

Our multiwavelength data set has enabled us to make a number of suggestions as to what took place during the outburst of GS 1354−64 in 1997 November. The optical and radio light curves suggest that there were two maxima during the outburst, the first prior to our observations and the second at ∼JD 245 0784, depending on wavelength. There is also the hint of a third optical rise just following the X-ray peak (JD 245 0796) – by this time it is possible that the disc is sufficiently bright in X-rays for the third optical brightening to be the result of X-ray reprocessing in the disc (although this is not confirmed by the hard X-ray energy spectrum). For future outbursts, simultaneous X-ray and high time-resolution optical observations would be extremely beneficial; discovery of the mHz QPO (mentioned in Section 3.1) in the optical would help to determine the efficiency of the reprocessing of soft X-rays.

It is clear that the optical light curve reached a local maximum *before* the X-rays peaked. While common in dwarf novae outbursts, a preceding optical peak is not generally seen in X-ray transient events – quite possibly only due to the fact that it is the X-ray satellites which tend to discover them. If this is the case, then it is unlikely that reprocessing of X-rays was the dominant source of optical emission. [However, it is possible if there is some non-straightforward disc geometry, e.g., GRO J1655−40 (Hynes et al. 1998).] Our comparison of 'soft' X-ray transients which remain in the low/hard X-ray state for the duration of the outburst shows that GS 2023+338 and possibly GRO J0422+32 were also observed to peak in the optical before the X-ray. While this may be coincidence in timing of the observations, we consider the

possibility that in these hard-state transients the X-ray emission is at a sufficiently low level for the inwards travelling instability to dominate the optical emission; in outbursts with a soft X-ray component reprocessing of X-rays would dominate instead. This is confirmed by the surprisingly high optical/X-ray luminosity ratios that these low/hard state sources have – in a 'normal' soft event the relative X-ray luminosity would be much higher than in the hard-state sources.

If the peak of the X-ray light curve corresponds to the time at which the instability reaches the hot inner regions of the disc, then a disc-crossing time of $\sim$10 d is inferred. For this to be true, the disc and therefore the orbit must be large. The fact that no orbital period has been determined for this source also suggests that the orbit may be large (this may also contribute to the possible over-bright optical emission mentioned in Section 3.2) – although it is more likely that there are insufficient optical data for any periodicities to be determined. If indeed the orbit *is* large, then BW Cir would have to be an evolved star filling its Roche lobe, suggesting a similar type of system to GRO J1655−40.

This inferred disc-crossing time is very long, and it is unlikely that the disc of a system with such a low soft X-ray luminosity and hard X-ray spectrum would extend to a small inner radius. It is also unlikely that the instability could trigger a radio ejection before reaching the innermost regions of the disc and causing the X-ray peak. The increase in QPO frequency suggests that the increase in soft X-ray luminosity is the result of the inner disc radius decreasing; the surface area of the disc and the temperature of the inner regions are therefore increasing. This would be consistent with other X-ray binaries – the low/hard state is characterized by a large inner disc radius, and this decreases on transition to the high/soft state (e.g. Esin et al. 1998).

Therefore it appears that the instability moves inwards, emitting in the optical regime. As the transported mass fills the 'hole' at the centre of the disc on a viscous time-scale, the soft X-ray emission from the corona increases. This scenario is comparable with that suggested by Shahbaz et al. (1998) to explain the optical/X-ray delay of the 1997 outburst of the neutron star X-ray transient Aql X-1.

If we assume that a radio event is triggered when the instability reaches the inner edge of the disc, then this considerably reduces the required disc crossing time (i.e., the disc crossing time becomes the delay between the optical and radio peaks rather than the delay between the optical and X-ray) and seems more likely. From observations of other sources in the hard state it is probable that the first radio event is a discrete ejection, with relativistic bulk velocity, which rapidly evolves to an optically thin spectrum. Subsequently, in the low/hard state, a powerful, steady, partially self-absorbed jet is produced which is observed approximately as a flat-spectrum component (Fender 2001b). It is also possible that repeated discrete ejections take place – however, these are more commonly seen in the soft X-ray transient outbursts and do not seem to be a common feature of the low/hard X-ray state.

Alternatively (or additionally?), we also note that the optical and radio data have comparable fluxes. It is therefore possible that an ejection event took place, emitting synchrotron radiation at optical and increasingly longer wavelengths as the ejected material became optically thin at increasing distances from the central source. The flat spectrum (Fig. 5), apparently extending from radio wavelengths to the *R* band, would certainly support this scenario. If, as our value of ξ suggests, the optical component is over-bright, then synchrotron should not be discounted as a possible contributor to the optical emission in addition to the thermal disc spectrum.

It is important to consider the implications of a jet (or mass ejection) that emits flat spectrum synchrotron radiation over such a wide range of frequencies. While there are a number of models that work reasonably well for the 'flat-spectrum' AGN, none of these is consistent with the *much flatter* radio – (sub)mm spectra of, e.g., Cyg X-1, GRS 1915+105 and Cyg X-3 (Fender et al. 2000, and references therein). The most convincing explanation for the flat spectrum is synchrotron radiation from a partially self-absorbed jet. With the power of the jet directly proportional to the bandwidth, detection of a high-frequency cut-off to the flat spectrum would be very useful in determining the power of the jet – this has not been found in any of the flat-spectrum X-ray binaries.

In summary, our limited observations suggest that the 1997 outburst of GS 1354−644 was the result of an instability crossing the disc on a slow viscous time-scale, emitting at optical wavelengths. As the instability reached the (large) inner radius of the disc, it triggered a mass ejection which emitted synchrotron radiation at radio wavelengths and possibly through to the near-infrared (and optical?) regime. The X-ray source remained in the low/hard state throughout, gradually becoming brighter as the instabilities carried more matter into the hot inner regions and subsequently decreasing the inner disc radius. These results clearly reflect the importance of simultaneous optical, infrared and radio studies of future X-ray transient events.

ACKNOWLEDGMENTS

This work was completed on the Sussex Starlink node. We are very grateful for the quick-look results provided by the *ASM*/RXTE and *CGRO*/BATSE teams, and to the various people who have taken observations for us. The Australia Telescope is funded by the Commonwealth of Australia for operation as a National Facility managed by CSIRO. We are also grateful to Ben Stappers, Jörn Wilms and Guillaume Dubus for useful conversations.

CB acknowledges a PPARC studentship; PGJ and PJG are supported by NWO Spinoza grant 08-0 to E. P. J. Van den Heuvel. PJG is also supported by a CfA Fellowship.

REFERENCES

Belloni T., Hasinger G., 1990, A&A, 227, L33
Brocksopp C., Fender R. P., Larionov V., Lyuty V. M., Tarasov A. E., Pooley G. G., Paciesas W. S., Roche P., 1999, MNRAS, 309, 1063
Buxton M., Vennes S., Ferrario L., Wickramasinghe D. T., 1998, IAU Circ. 6815
Callanan P. J. et al., 1995, ApJ, 441, 786
Cardelli J. A., Clayton G. C., Mathis J. S., 1989, ApJ, 345, 245
Castro-Tirado A. J., Ilovaisky S., Pederson H., 1997, IAU Circ. 6775
Charles P. A., 1998, in Abramowicz M., Bjornsson G., Pringle J., eds, Theory of Black Hole Accretion Disks. Cambridge Univ. Press, Cambridge, p. 1
Chen W., Shrader C. R., Livio M., 1997, ApJ, 491, 312
Corbel S., Fender R. P., Tzioumis A. K., Nowak M., McIntyre V., Durouchoux P., Sood R., 2000, A&A, 359, 251
Cui W., Zhang S. N., Focke W., Swank J. H., 1997, ApJ, 484, 383
Cui W., Barret D., Zhang S. N., Chen W., Boirin L., Swank J., 1998, ApJ, 502, L49
Dhawan V., Pooley G. G., Ogley R. N., Mirabel I. F., 2000, IAU Circ. 7395
Ebisawa K. et al., 1994, PASJ, 46, 375

Esin A. A., Narayan R., Cui W., Grove J. E., Zhang S. N., 1998, ApJ, 505, 854
Fender R. P., 2001a, in Kaper L., Van den Heuvel E. P. J., Woudt P. A., eds, To be published in Proc. ESO workshop Black Holes in binaries and galactic nuclei. Springer-Verlag
Fender R. P., 2001b, MNRAS, 322, 31
Fender R. P., Tingay S. J., Higdon J., Wark R., Wieringa M., 1997, IAU Circ. 6779
Fender R. P. et al., 1999, ApJ, 519, L165
Fender R. P., Pooley G. G., Durouchoux P., Tilanus R. P. J., Brocksopp C., 2000, MNRAS, 312, 853
Fishman G. J. et al., 1989, in Johnson W. N., eds, Proc. GRO Science Workshop. NASA, p. 96
Francey R. J., 1971, Nature Phys. Sci., 229, 228
Frank J., King A., Raine D., 1992, Accretion Power in Astrophysics. Cambridge Univ. Press, Cambridge, Chap 5
Garcia M., Brown W., Pahre M., McClintock J., Callanan P., Garnavich P., 2000, IAU Circ. 7392
Han X., Hjellming R. M., 1992, ApJ, 400, 304
Harmon B. A., Robinson C. R., 1997, IAU Circ. 6774
Hjellming R. M., Han X., Roussel-Dupre ., 1990, IAU Circ. 5112
Hjellming R. M., Rupen M. P., Shrader C. R., Campbell-Wilson D., Hunstead R. W., McKay D. J., 1996, ApJ, 470, L105
Hjellming R. M. et al., 1999, ApJ, 514, 383
Homan J., Wijnands R., Van der Klis M., Belloni T., Van Paradijs J., Klein-Woldt M., Fender R. P., Méndez M., 2000, ApJS, in press (astro-ph/0001163)
Hynes R. I., 1998, New Astronomy Reviews, 42, 605
Hynes R. I., O'Brien K. O., Horne K., Chen W., Haswell C. A., 1998, MNRAS, 299, L37
Hynes R. I., Mauche C. W., Haswell C. A., Shrader C. R., Cui W., Chaty S., 2000, ApJ, 299, L37
Jahoda K., Swank J. H., Giles A. B., Stark M. J., Strohmayer T., Zhang W., Morgan E. H., 1996, SPIE, 2808, 59
Kitamoto S., Tsunemi H., Pedersen H., Ilovaisky S. A., Van der Klis M., 1990, ApJ, 361, 590
Kouveliotou et al., 1992, IAU Circ. 5592
Kuulkers E., Fender R. P., Spencer R. E., Davis R. J., Morison I., 1999, MNRAS, 306, 919
Landolt A. U., 1992, ApJ, 140, 340
Levine A. M., Bradt H., Cui Wei Jernigan J. G., Morgan E. H., Remillard R., Shirey R. E., Smith D. A., 1996, ApJ, 469, L33
Makino F. et al., 1987, IAU Circ. 4342,
Markert T. H. et al., 1979, ApJS, 39, 573
Méndez M., Belloni T., Van der Klis M., 1998, ApJ, 499, 187
Orosz J., 1997, ApJ, 477, 876
Psaltis D., Belloni T., Van der Klis M., 1999, ApJ, 520, 262
Reig P., Méndez M., Van der Klis M., Ford E. C., 2000, ApJ, 530, 916
Remillard R., Marshall R., Takeshima T., 1997, IAU Circ. 6772
Revnivtsev M. G., Borozdin K., Priedhorsky W. C., Vikhlinin A., 2000, ApJ, 530, 955
Shahbaz T., Bandyopadhyay R. M., Charles P. A., Wagner R. M., Muhli P., Hakala P., Casares J., Greenhill J., 1998, MNRAS, 300, 382
Shrader C. R., Wagner R. M., Hjellming R. M., Han X. H., Starrfield S. G., 1994, ApJ, 434, 698
Soria R., Bessell M. S., Wood P., 1997, IAU Circ. 6732,
Sunyaev R. A. et al., 1993, A&A, 280, L1
Swinbanks D., 1987, Nat, 326, 322
Tanaka Y., Lewin W. H. G., 1995, in Lewin W. H. G., Van Paradijs J., Van den Heuvel E., eds, X-Ray Binaries. Cambridge Univ. Press, Cambridge
Tanaka Y., Shibazaki N., 1996, ARA&A, 34, 607
Van der Hooft F. et al., 1996, ApJ, 458, L75
Van der Hooft F. et al., 1999, ApJ, 513, 477
Van der Klis M., 1994, A&A, 283, 469
Van der Klis M., 1995, in Lewin W. H. G., Van Paradijs J., Van den Heuvel E., eds, X-Ray Binaries. Cambridge Univ. Press, Cambridge
Van Paradijs J., 1996, ApJ, 464, L138
Van Paradijs J., 1998, in Buccheri R., Van Paradijs J., Alpar M. A., eds, The Many Faces of Neutron Stars. Kluwer Academic Publishers, Dordrecht
Van Paradijs J., McClintock J. E., 1995, in Lewin W. H. G., Van Paradijs J., Van den Heuvel E., eds, X-Ray Binaries
Vikhlinin A. et al., 1994, ApJ, 424, 395
Wood K. S. et al., 2000, ApJ, 544, L45
Yamaoka K., Ueda Y., Dotani T., Durouchoux P., Rodriguez J., 2000, IAU Circ. 7427
Życki P. T., Done C., Smith D. A., 1999, MNRAS, 309, 561

This paper has been typeset from a TEX/LATEX file prepared by the author.